Journal of Colloid and Interface Science 350 (2010) 453–458

Contents lists available at ScienceDirect

Journal of Colloid and Interface Science

www.elsevier.com/locate/jcis

Immobilization of genetically engineered fusion proteins on gold-decorated carbon nanotube hybrid films for the fabrication of biosensor platforms

HoSeok Park [a], Tae Jung Park [b,*], Yun Suk Huh [c], Bong Gill Choi [d], Sungho Ko [e], Sang Yup Lee [b,d], Won Hi Hong [d,**]

[a] Department of Chemical Engineering, Kyung Hee University, 1 Seocheon-dong, Giheung-gu, Yongin-si, Gyeonggi-do 446-701, Republic of Korea
[b] BioProcess Engineering Research Center, Center for Systems & Synthetic Biotechnology, Institute for the BioCentury, KAIST, Daejeon 305-701, Republic of Korea
[c] Division of Materials Science, Korea Basic Science Institute, Daejeon 305-333, Republic of Korea
[d] Department of Chemical & Biomolecular Engineering (BK21 Program), KAIST, Daejeon 305-701, Republic of Korea
[e] Korea Food Research Institute, 516 Baekhyun-dong, Bundang-gu, Seongnam 463-746, Republic of Korea

ARTICLE INFO

Article history:
Received 25 May 2010
Accepted 23 June 2010
Available online 30 June 2010

Keywords:
Carbon nanotube
Gold nanoparticle
Fusion protein
Electrode
Biosensor

ABSTRACT

We have demonstrated the fabrication of the biosensor platforms by means of the integration of the genetically engineered fusion proteins and the uniform gold nanoparticle-deposited multi-walled nanotube hybrid (Au-MWNT-HB) films for the detection of C-reactive protein (CRP). Au-MWNT-HB films were used as a good electrochemical transducer due to their excellent electrical properties and large surface areas for the signal transduction, while the genetically engineered fusion proteins, or 6His–GBP–SpA fusion proteins, specifically bind onto the surface of the Au-MWNT-HB films and efficiently immobilize bioreceptors for the detection of CRP. As-obtained biosensor platforms were characterized by electrochemical and optical analysis and revealed better performance compared to conventional Au-based biosensors. The concept delineated herein opens a new insight into nanobiotechnology through the integration of genetically engineered biomaterials with carbon nanotube (CNT)-based nanohybrids for emerging applications.

1. Introduction

The integration of nanomaterials and biomolecules is one of the most significant and interesting challenges in interdisciplinary nanobiotechnologies [1]. From a practical point of view that the former provides excellent electrical, optical, and magnetic properties while the latter possesses unique biological functionalities, this fusion technology is expected to broaden its applications in an emerging class of fields, including sensing, imaging, catalysis, electronics, and cell targeting [2]. Herein, we first the fabrication and characterization of emerging biosensing platforms which are integrated by uniformly gold nanoparticle-deposited multi-walled nanotube hybrids (Au-MWNT-HBs) with genetically engineered fusion proteins for the detection of C-reactive protein (CRP).

Carbon nanotube (CNT)–nanoparticle (NP) hybrids have received significant attention as an emerging class of nanomaterials with desirable properties for multifunctional applications, such as optoelectronics, catalysis, sensors, and hydrogen or power storage [3]. In particular, hybridization of CNTs with Au NPs has been intensively investigated to fabricate highly efficient sensor devices due to large surface area, favorable electronic properties, ease of biomolecule attachment, and electrocatalytic effects [4]. Despite these advantages for applications into electrochemical transducers, however, surface modification is further required to immobilize bioreceptors on the sensor platforms based on CNT-Au electrodes. In this regard, the integration of nanomaterials and fusion proteins are suggested as a new method for the development of electrochemical sensor platforms [5].

Molecular biomimetics, inspired by biological structures and functions, are a hybrid technology, as it synergistically combines the tools of biotechnology and nanotechnology [5]. Recently, these elegant and sophisticated methodologies have been driven into the development of genetically engineered polypeptides (GEPs) for a wide range of applications in material science and nanobiotechnology [5,6]. Some of GEPs can specifically bind onto the surfaces of various organic and inorganic materials with high affinity. Amongst a variety of GEPs, gold binding polypeptides (GBPs) that uniquely interact with the Au lattice take an advantage over typically physical and chemical methods to modify the surface characteristics of biosensor platform in terms of hybridizing nanomaterials and biomolecules through biologically well-programmed assembly [7]. Especially, the special functionalities or

* Corresponding author. Fax: +82 42 350 8800.
** Corresponding author. Fax: +82 42 350 3910.
E-mail addresses: tjpark@kaist.ac.kr (T.J. Park), whhong@kaist.ac.kr (W.H. Hong).

0021-9797/$ - see front matter © 2010 Elsevier Inc. All rights reserved.
doi:10.1016/j.jcis.2010.06.058

molecular recognitions can be also introduced into GEPs with task-specific proteins, resulting in the broadening of applicative fields.

In this study, we developed a simple method for the immobilization of fusion protein as a functional bioreceptor on the Au-MWNT-HB films; genetically engineered GBP-fusion protein was employed as a biolinker with the high affinity against the Au surface and fused with Staphylococcal Protein A (SpA) acting as a capture ligand for antibody binding [6,7]. The basic strategy described here is: (1) to use the Au-MWNT-HBs as an electrochemical substrate based on their excellent electrical properties and large surface areas for the immobilization of bioreceptors and (2) to fabricate a sensing platform by using 6His–GBP–SpA fusion protein, where GBP specifically binds onto the surface of the Au-MWNT-HBs and anti-CRP linked with SpA selectively detects CRP through the antibody–antigen interactions.

2. Materials and methods

2.1. Preparation of 6His–GBP–SpA fusion protein

Six histidine (6His) residues were introduced to facilitate purification of fusion proteins by metal affinity chromatography. The DNA fragment encoding incomplete 6His–GBP was first obtained by polymerase chain reaction (PCR) amplification using the primers P1 (5′- GAAACAGCATATGCACCATCACCATCACCACCACGGCAAA ACCCAGGCGACCAG -3′) and P2 (5′- GGAATTCAGACTGAATGG TACCGCTCGTCGCTTGGGTTTTACCGTGCATAGATT -3′), and the plasmid pTGE as a template. Then, the primers P3 (5′- GGAATTCGCG CAACACGATGAAGCTCAA -3′) and P4 (5′- AGGGATCCTTATAGTTCG CGACGACGTCC -3′) were used to amplify the *spa* gene fragment encoding the SpA using the genomic DNA of *Staphylococcus aureus* Mu50 (ATCC 700699D) as a template. The PCR product of the 6His–GBP was digested with *Nde*I and *Eco*RI, and the PCR product of the SpA was digested with *Eco*RI and *Bam*HI. Then, they were ligated into *Nde*I and *Bam*HI sites of pET-22b(+) to make pET-6HGBP-SpA(Mu50).

For the production of 6His–GBP–SpA fusion protein, *Escherichia coli* BL21(DE3) (F^- *ompT hsdS*$_B$ (rB^- mB^-) *gal dcm* (DE3)) harboring pET-6HGBP-SpA(Mu50) was cultivated in 100 mL Luria–Bertani medium (10 g/L tryptone, 5 g/L yeast extract, 5 g/L NaCl) supplemented with ampicillin (100 μg/mL) in a shaking incubator at 37 °C and 200 rpm. After addition of isopropyl-β-D-thiogalactopyranoside, cells were further cultivated for 6 h. Cells were harvested and disrupted by sonication for 1 min at 20% output power. After centrifugation at 16,000*g* for 10 min at 4 °C, the pellet containing the soluble protein fraction was saved for the purification of fusion proteins. Ni–NTA column was used for the purification of the fusion proteins without further purification steps.

2.2. Fabrication of biosensor platforms

To synthesize Au-MWNT-HBs, MWNTs of 2 mg were mixed with 1-butyl-3-methylimidazolium tetrafluoroborate (C_4MimBF_4) of 0.4 mL, and the mixture was ground with an agate mortar for 20 min; the suspension gradually turned into a glossy, black paste. The resulting paste was washed repeatedly with acetonitrile and deionized (DI) water to remove excess $BMimBF_4$ and dried under vacuum at 40 °C to yield MWNT–C_4MimBF_4 hybrids. MWNT–C_4MimBF_4 of 1 mg was mixed with 4×10^{-3} mmol of $HAuCl_4{\cdot}3H_2O$ in ethanol of 2 mL and DI water of 2 mL. The resulting mixtures were sonicated for 30 s (Branson 3510, 42 kHz). It resulted in the growth and decoration of Au NPs on the surfaces of MWNT–C_4MimBF_4. After washing Au-MWNT-HBs with deionized water, they were filtrated and then dried under vacuums at 40 °C.

To fabricate homogeneous CNT films [8], Au-MWNT-HBs of 1.5 mg were dispersed in 200 mL of dimethylformamide (DMF). The resulting solution was filtrated by anodic aluminum oxide (AAO) membrane with pore size of 0.02 μm (Anodisc 47, Whatman®) under vacuums. Then, Au-MWNT-HBs coated AAO membrane was directly placed into a bath of 3 M NaOH. The AAO membrane was gradually dissolved and Au-MWNT-HB films were transferred onto the glass substrate. The NaOH solution was exchanged with DI water by recirculation until the pH became near 7.0. The electrode was patterned by using the evaporation of 5 nm Ti/50 nm Au and the shadow mask, and deposited on the Au-MWNT-HB coated glass.

2.3. Electrochemical characterization for the detection of CRP

CRP and anti-CRP polyclonal antibody were purchased from Fitzgerald (Concord, MA). For the detection of CRP, GBP-fusion protein solution of 20 μL in PBS at the concentration of 50 μg/mL was dropped onto Au-MWNT-HB films and washed by DI water. Likewise, after drying Au-MWNT-HB films coated with 6His–GBP–SpA fusion protein, anti-CRP solution of 20 μL in PBS at the concentration of 50 μg/mL was dropped onto them and also washed by DI water. Finally, CRP solution of 20 μL in PBS in the concentration range of 100 ng/mL−15 μg/mL was dropped onto 6His–GBP–SpA and anti-CRP immobilized Au-MWNT-HB films, washed with DI water, and dried. In order to improve the reproducibility of biosensors, the content of Au NPs was fixed to ~7 wt.% by controlling the concentration of NP precursors. Furthermore, the concentration of GBP-fusion protein immobilized on the surface of Au NPs was controlled to guarantee the absence of an excess amount. Consequently, all results were averaged in the error range of ±5.5%.

2.4. Instrumental methods

Biosensor platforms were characterized by transmission electron microscopy (TEM), high resolution TEM (HR-TEM), scanning TEM (STEM), SEM, surface plasmon resonance (SPR), SPR imaging (SPRi), and cyclic voltammetry (CV). TEM images were collected on an E.M. 912 Ω energy-filtering TEM (EF-TEM, 120 kV) and a JEM-3010 HR-TEM (300 kV). A STEM was operated with a probe focused to 0.2 nm and camera length of 20 cm. The scan raster was 512×512 points with a dwell time of 8.5 s per scan. SEM images were obtained by a Field Emission Scanning Electron Microscope (Philips SEM 535 M) equipped with Schottky-based field emission gun. An SPR analysis (AutoLab, Utrecht, Netherlands) was performed at a flow rate of 5 μL/min on the bare gold chip. Also, SPRi analysis was carried out by using a SPRi instrument (K-MAC, Daejeon, Korea) with an incoherent light source (a 150 W quartz tungsten–halogen lamp, Scott, Mainz, Germany) for excitation. Reflected light from this assembly was passed *via* a bandpass filter-centered at a wavelength of 830 nm and collected by a CCD camera (Sony, Tokyo, Japan). Data images were collected digitally *via* a B/W frame grabber. Scion Image release Beta 4.0.3 software (Scion Corp., Frederick, MD) was used to analyze the images. The bare Au chip (25 mm × 25 mm × 1 mm) on glass was assembled on the SPRi system by attaching a silicon packing with a thickness of 20 mm between the gold-layered-cover glass and a prism of the SPR detector. Matching oil with a refractive index of 1.516 was coated between the backside of the cover glass of the sensor chip and the prism. Bulk refractive index change and non-specific binding were not compensated. All measurements were performed in an air-conditioned room at 24–26 °C. The SPRi difference images were produced by subtracting a reference image from a post-binding image, contributing to visual confirmation of binding. The brighter spots indicate binding of the target proteins onto the gold surface because reflectivity increases when binding occurs. CV was

carried out to analyze the electrochemistry of biosensor platforms integrated by Au-MWNT-HBs and GBP-fusion protein for the detection of CRP. Ferrocenemethanol of 0.5 mM in PBS was used as a supporting electrolyte. The electrochemical CV scans were recorded using a CHI 660C electrochemical workstation (CH Instruments, Austin, TX) with a conventional three-electrode electrochemical slide using a gold working electrode, a KCl saturated silver–silver chloride (Ag/AgCl) reference electrode and a platinum wire counter electrode, respectively. All potentials were herein collected versus a standard saturated Ag/AgCl electrode. The potential was applied to the sensor at the scan rate of 50 mV/s, and the current proportional to the concentration of the electroactive species was measured. The measured current at the working electrode was the response of the CV. A peak was also observed in the reverse scan; this peak resulted from the electrochemical reaction of intermediates or products of the reactions during the forward scan. Separation of the anodic and cathodic current peaks could be used to predict the number of electrons involved in the redox reaction. Repeated cycles of reduction and oxidation of the analyte generated alternating anodic and cathodic currents in and out of the working electrode. Experimental results were plotted as potential versus current.

3. Results and discussion

3.1. Fabrication of electrochemical biosensor platforms

Fig. 1 illustrates the procedures of fabricating biosensor platforms for the targeting of CRP. First, Au-MWNT-HBs were synthesized *via* an ionic liquid-assisted sonochemical method (ILASM). This novel technique integrates the supramolecular assembly of CNTs and ionic liquids (ILs) with sonochemistry to form CNT–metal HBs in which the well-defined NPs are attached to the surfaces of CNTs [9]. Fig. 2 shows TEM and STEM images of Au-MWNT-HBs. Discrete Au NPs, which were synthesized in situ and decorated onto the surface of ionic liquid-wrapped MWNT, had a size distribution of 5.23 ± 1.32 nm. HR-TEM images of the Au-MWNT-HBs revealed lattice resolved fringes of the Au, indicating the formation of nanocrystalline structure. The presence and uniform distribution of the Au NPs deposited onto the sidewall of MWNTs were analyzed by the signals of the Au and carbon in STEM images (~7 wt.% of the Au from EDS analysis of Fig. 1b and Fig. S1). Second, the homogeneous films of the Au-MWNT-HBs were prepared through a directional flow-induced assembly for the patterned electrode [8]. The well-interconnected CNT networks of Au-MWNT-HB films provide many activated sites to the Au for the immobilization of GBP-fusion protein as a bioreceptor as well as percolated conduction pathways for the charge transfer (see Fig. S2). Third, 6His–GBP–SpA fusion protein in phosphate-buffered saline (PBS, pH 7.4) solution was specifically bound to the Au NPs of Au-MWNT-HB films through the specific interactions between Au NPs and GBPs. In order to detect CRP on the CNT hybrid-fusion protein biosensors, anti-CRP antibody was incorporated into the biosensor platform by interacting with the SpA protein.

3.2. Electrochemical behavior of biosensor platforms

To demonstrate the usefulness of Au-MWNT-HB and GBP region of the fusion protein (GBP-segment) for the electrochemical sensing, the electrochemical detection tests of CRP were performed. The electrochemical behavior of Au-MWNT-HB films was presented to assess the applicability as a platform of the electrochemical biosensor. Fig. 3a presents CV curves of Au-MWNT-HB films in N_2-saturated PBS solution at the scan rates of 25–500 mV/s. The current signals and peak-to-peak potential separation (ΔE_p) were increased as a function of scan rate. In particular, Au-MWNT-HB films revealed the linear relationship of I_p versus $v^{1/2}$, which follows the Randles–Sevčik equation below [10]:

$$I_p = 0.4463\left(\frac{F^3}{RT}\right)^{1/2} n^{3/2} A D_o^{1/2} C_o v^{1/2} \quad (1)$$

where I_p is the peak current, n is the number of charge, A is the area of the interface, D_o is the diffusion coefficient of the transferred species, C_o is the concentration, and υ is the scan rate.

As shown in Fig. 3b, a perfect scaling of steady state currents in Au-MWNT-HB electrodes (r^2 is 0.997 and 0.998 for I_{pa} and I_{pc}, respectively) suggests that the interfacial behavior was governed by the diffusion controlled system of electroactive components in the process of adsorption and desorption, so called Nernstian or reversible systems [11]. However, further studies by impedance spectra should be performed to confirm the diffusion controlled system.

The changes in the current signals by the immobilization of CRP should be clarified to define the detection range of Au-MWNT-HB film based biosensors. All CV curves of Au-MWNT-HB films for

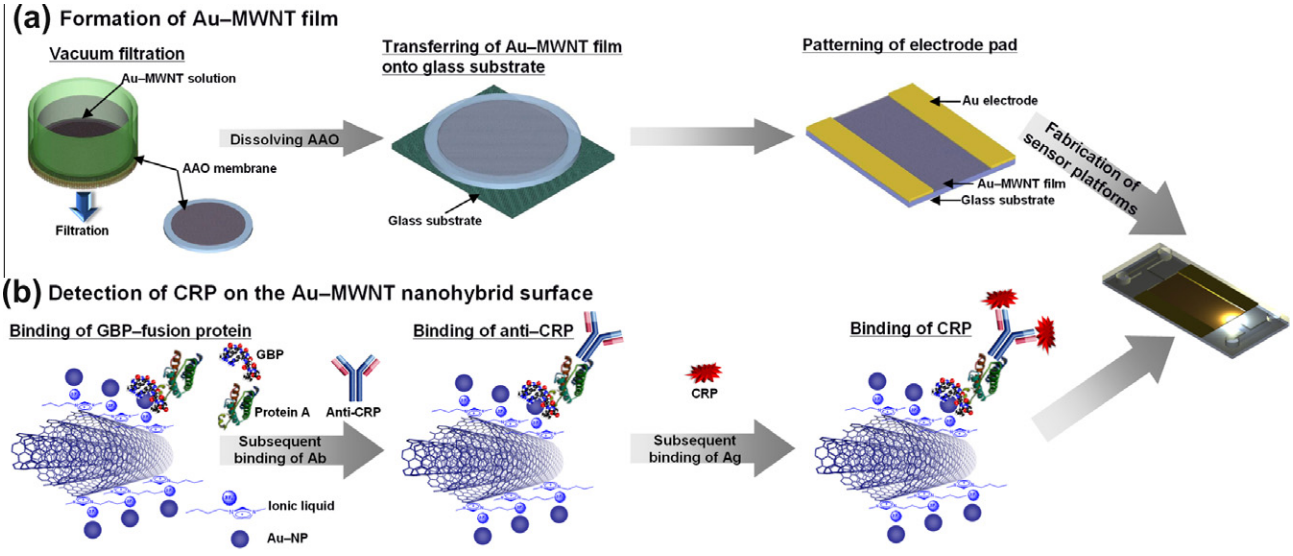

Fig. 1. Illustration for the procedures of preparing biosensor platforms for the CRP targeting.

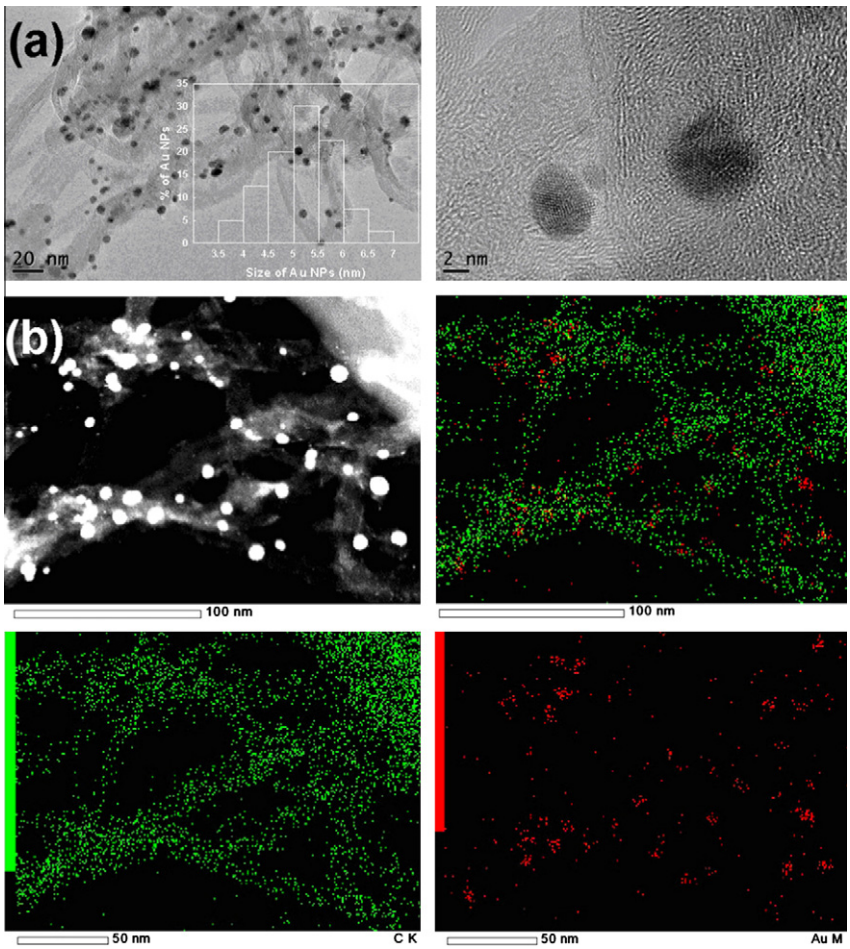

Fig. 2. (a) TEM and HR-TEM images and (b) STEM image of the Au-MWNT-HBs. Inset of 2a represents the size distribution of Au NPs. STEM image: TEM dark field image (left up), mass mapping of mixed C and Au (right up), C (left down, green spot), and Au (right down, red spot). (For interpretation of the references to colour in this figure legend, the reader is referred to the web version of this article.)

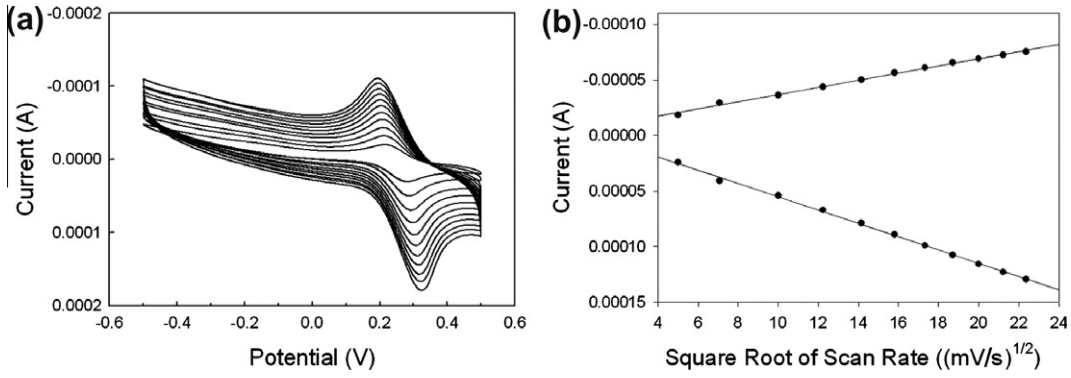

Fig. 3. (a) Cyclic voltammograms and (b) linear relationship of I_p and square root of scan rate ($v^{1/2}$) of Au-MWNT-HB films at the scan rates of 25–500 mV/s (supporting electrolyte: 0.5 mM ferrocenemethanol in PBS). Circles indicate oxidation values, while triangles represent reduction signals.

the CRP detection were obtained at the concentration range of 100 ng/mL–15 μg/mL as shown in Fig. 4. The changes in the current signals were observed down to 100 ng/mL which was ~10-fold lower than the typical clinical cutoff concentration of 1 μg/mL. Several groups have demonstrated higher sensitivities of <100 ng/mL [12], but additional steps for the functionalization of transducer materials are required to immobilize biomarkers. Furthermore, the linear detection range of CRP was observed from 2.5 to 15 μg/mL (r^2 is 0.9488 and 0.9518 for oxidation and reduction, respectively).

In comparison to current–voltage (IV) curves of C_4MimBF_4-wrapped MWNT, Au-MWNT-HB films exhibited lower current signals due to the significant enhancement of resistance after the binding of CRP to the anti-CRP at the drying state (see Fig. S3). In a similar manner to the resistor type-device based on CNT [13], the modulation of electrical conductance in this device was attributed not to CNT–metal electrode junction but to the changes in the resistances, by means of the adsorption of biomolecules. In order to investigate the effect of the Au NPs on the performance for the detection of CRP, CV curves of the bare Au and Au-MWNT-HB were

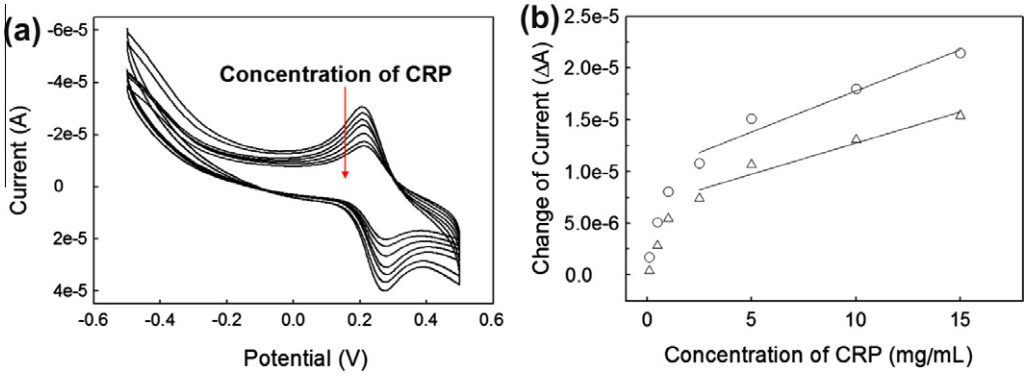

Fig. 4. (a) Cyclic voltammograms of Au-MWNT-HB films at various CRP concentrations range from 100 ng/mL to 15 μg/mL in PBS solution containing 0.5 mM ferrocenemethanol and (b) plots of CRP concentration and changes of peak current showing the difference of peak currents as a reference of Au-MWNT-HB films without CRP loading. Circles indicate oxidation values, while triangles represent reduction signals.

measured after the sequential immobilization of 6His–GBP–SpA fusion protein, anti-CRP, and CRP, as shown in Fig. 5. Au-MWNT-HB films exhibited more significant changes of the current and ΔE_p compared to the bare Au, because of the high ratio of surface area to volume and facile accessibility to activated sites by means of the discrete Au NPs. The binding sites, which are provided by Au NPs of nanohybrids, promoted the specific immobilization of GBP-SpA fusion protein, anti-CRP, and CRP, respectively. The oxidation peaks of ferrocenemethanol in Au-MWNT-HB films were significantly shifted due to the specific interactions of the Au NPs and GBP-fusion protein. Furthermore, the absence of any semi-circle in Nyquist plot indicates the close contact between the Au-MWNT-HB electrode and the electrolyte through the low interfacial resistance (see Fig. S4) [9,10]. The favorable interfacial characteristics are related to the electronic equilibrium of hybrid materials *via* energy transfer among MWNT, C_4MimBF_4 and Au NP [9,10]. Therefore, Au-MWNT-HB films are suitable to the electrochemical transducer due to the facilitated charge transfer by means of good interfacial properties and discrete Au NPs.

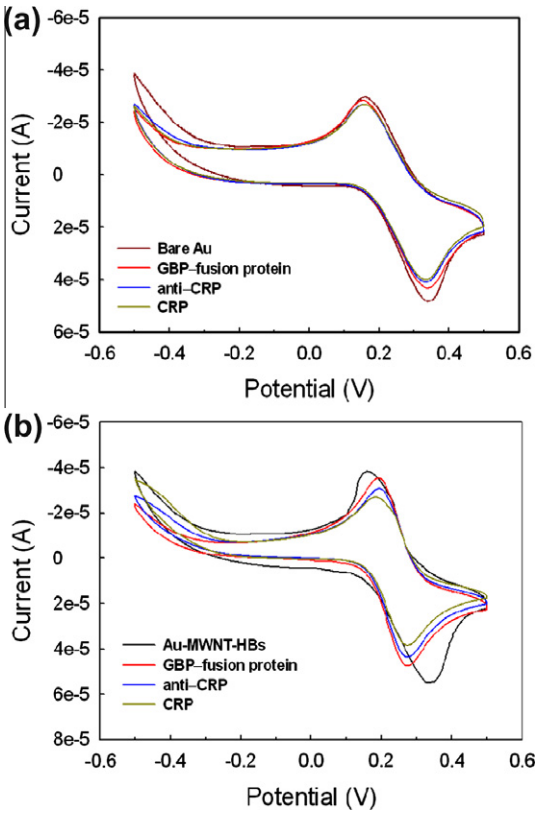

Fig. 5. Cyclic voltammograms of (a) bare Au and (b) Au-MWNT-HB films after the sequential deposition of 6His–GBP–SpA (50 μg/mL), anti-CRP (50 μg/mL), and CRP (100 ng/mL) (supporting electrolyte: 0.5 mM ferrocenemethanol in PBS, scan rate: 50 mV/s).

3.3. Binding behavior of CRP on sensing platforms

To verify the binding specificity of biosensor platforms consisting of Au-MWNT-HBs and GBP-fusion proteins by optical analysis, SPR detection experiments were performed. Fig. 6 presents SPR sensorgrams on the Au surface. BSAs were used to prevent non-specific binding, while residual fusion protein, anti-CRP, and CRP were removed by washing step. The intensities of SPR were concomitantly enhanced with the sequential bindings of 6His–GBP–SpA, anti-CRP, and CRP on the Au surface. In contrast, a control sample without CRP did not reveal the enhancement of SPR intensity (dotted line). These results elucidate that 6His–GBP–SpA fusion proteins specifically bind onto the Au surface and effectively immobilize anti-CRP and CRP, subsequently, due to the specific interactions between GBP and Au, SpA and anti-CRP, and anti-CRP and CRP, respectively. In order to explore the effectiveness of the Au-MWNT-HBs on the sequential bindings of 6His–GBP–SpA fusion protein, anti-CRP, and CRP, SPRi analyses of the modified electrode were compared to those of the bare Au electrode. As shown in SPRi, both spot intensities of the bare Au and Au-MWNT-HB micropatterns were subsequently increased by the sequential bindings of GBP-SpA fusion protein, anti-CRP, and CRP. The spots were concomitantly brightened in the course of reaction progress. These findings indicate that the interactions between the GBP-fusion protein and Au-MWNT-HB as well as between antigen and antibody are highly specific. Considering that the contrast of the Au-MWNT-HB-coated electrode was more apparent than that of the bare Au electrode, Au-MWNT-HBs serve as highly efficient transducer materials for the immobilization of bioreceptors.

4. Conclusions

In conclusion, the electrochemical biosensor platforms were prepared by integrating Au-MWNT-HBs with genetically engineered GBP-fusion proteins for the detection of target analytes. Sensing platforms were readily fabricated by the direct immobilization of bioreceptor onto the Au-MWNT-HB films; Au-MWNT-HBs acted as an electrochemical substrate due to their excellent electrical properties and large surface area for the specific immobilization of the biomolecules and the efficient signal transduction, while

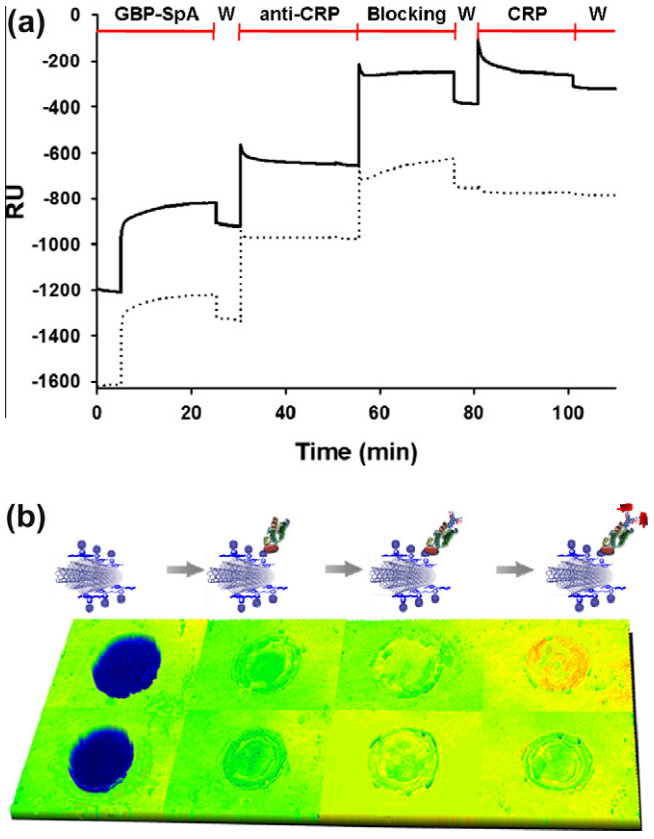

Fig. 6. (a) SPR sensorgrams on the surface of Au. Bold line, sample with 100 ng/mL of CRP; dotted line, control sample without CRP; GBP-SpA, 50 μg/mL of 6His–GBP–SpA fusion protein; W, washing step with PBS; anti-CRP, 50 μg/mL of polyclonal anti-CRP; Blocking, 100 μg/mL of BSA; CRP, 100 ng/mL of CRP and (b) SPRi images of Au-MWNT-HB coated electrode (middle) and the bare Au electrode (bottom) in the process of the subsequent immobilization of 6His–GBP–SpA, anti-CRP, and CRP (top); 50 μg/mL GBP-SpA; 50 μg/mL anti-CRP; 100 ng/mL CRP (from left to right).

GBP-fusion proteins, 6His–GBP–SpA fusion proteins, played a role of specifically binding onto the surface of the Au-MWNT-HBs as well as efficiently immobilizing bioreceptors for the selective CRP detection. The electrochemical properties of Au-MWNT-HBs were characterized by IV, CV, and impedance analysis, while the binding specialty of CRP on sensing platforms was verified by SPR and SPR imaging. As-obtained biosensor platforms revealed better performance compared to that of conventional Au-based biosensor by means of the combination of the 6His–GBP–SpA fusion proteins as a multifunctional bioreceptor and the Au-MWNT-HBs as an efficient electrochemical transducer. The GBP-SpA fusion protein simply and strongly self-immobilized onto the Au surface without any surface chemical modification could offer a stable and specific sensing platform for the target CRP detection *via* the anti-CRP binding. Furthermore, it suggests that a multiple detection can be designed since the bio-recognition elements against target analytes (e.g. antigen or antibody) can be easily fused with GBP *via* recombinant DNA technology. Finally, the linear detection range of CRP was shown from 2.5 to 15 μg/mL and the detection limit was down to 100 ng/mL which was ~10-fold lower than the clinical low-risk cut-off concentration for the cardiovascular monitoring. The sensitivity and dynamic range of this system can increase by applying enzyme-based immunoassay into the as-obtained devices. The integration of genetically engineered biomaterials with CNT-based nanohybrids paves the opportunities to develop new sensing platforms for biomedical applications with portable electrochemical devices.

Acknowledgments

This work was supported by the IT Leading R&D Support Project from the Ministry of Knowledge Economy (Korea) through KEIT and by WCU (World Class University) program through the National Research Foundation of Korea funded by the Ministry of Education, Science and Technology (R322009000101420).

Appendix A. Supplementary data

Supplementary data associated with this article can be found, in the online version, at doi:10.1016/j.jcis.2010.06.058.

References

[1] W. Jiang, E. Papa, H. Fischer, S. Mardyani, W.C.W. Chan, Trends Biotechnol. 22 (2004) 607.
[2] R.J. Tseng, C. Tsai, L. Ma, J. Ouyang, C.S. Ozkan, Y. Yang, Nat. Nanotechnol. 1 (2006) 72.
[3] G.G. Wildgoose, C.E. Banks, R.G. Compton, Small 2 (2006) 182.
[4] B. Wu, S. Hou, F. Yin, Z. Zhao, Y. Wang, X. Wang, Q. Chen, Biosens. Bioelectron. 22 (2007) 2854.
[5] M. Sarikaya, C. Tamerler, D.T. Schwartz, F. Baneyx, Annu. Rev. Mater. Res. 34 (2004) 373.
[6] M. Sarikaya, C. Tamerler, A.K.Y. Jen, K. Schulten, F. Baneyx, Nat. Mater. 2 (2003) 577.
[7] S. Brown, Nat. Biotechnol. 15 (1997) 269.
[8] Z.C. Wu, Z.H. Chen, X. Du, J.M. Logan, J. Sippel, M. Nikolou, K. Kamaras, J.R. Reynolds, D.B. Tanner, A.F. Herbard, A.G. Rinzler, Science 305 (2004) 1273.
[9] H.S. Park, B.G. Choi, S.H. Yang, W.H. Shin, J.K. Kang, D. Jung, W.H. Hong, Small 5 (2009) 1754.
[10] A.J. Bard, L.R. Faulkner, Electrochemical Methods. Fundamentals and Applications, second ed., John Wiley & Sons, New York, 2001.
[11] N.G. Shang, P. Papakonstantinou, M. McMullan, M. Chu, A. Stamboulis, A. Potenza, S.S. Dhesi, H. Marchetto, Adv. Funct. Mater. 18 (2008) 3506.
[12] K.W. Wee, G.Y. Kang, J. Park, J.Y. Kang, D.S. Yoon, J.H. Park, T.S. Kim, Biosens. Bioelectron. 20 (2005) 1932.
[13] X. Dong, D. Fu, Y. Xu, J. Wei, Y. Shi, P. Chen, L.J. Li, J. Phys. Chem. C 112 (2008) 9891.